Bimetallic Organic Frameworks for Wastewater remediation from Cr-Oxyanions

Mostafa Stoohi, Ahmed AbdElghafar, Yassen Alghobashy, AbdElfatah Ashraf, Omar Adel
Hesham Tantawy, Ahmad Baraka, and Osama Abuzalat*
Department of Chemical Engineering, Military Technical College, Cairo, Egypt
Email:osama.abuzalat@mtc.edu.eg

Abstract: ***The bimetallic metal organic framework (MOF), (Fe-Co)/BDC was synthesized via solvo-thermal method. PXRD, SEM/EDX, FTIR, Raman, XPS and BET were applied to characterize the as synthesized, (Fe-Co)/BDC. Characterization results reveals that (Fe-Co)/BDC MOF is flexible crystalline nano-porous material with significant anion exchange capability due to chloride resident-in-matrix anion. The evaluation of its adsorptive ion exchange against Cr-oxyanions was performed. Kinetic study applying pseudo first order (PFO), pseudo second order (PSO), diffusion-binding (DB), and Weber-Morris (WM) models suggests pseudo first order as suitable to represent the adsorption kinetics with diffusion is an effective step. Generally, Kinetic study revealed the speedy nature of of Cr-oxyanion adsorption with significant reversibility and simple regeneration by NaCl solution. Freundlich and Langmuir models were applied for isotherm study under isoelectric condition, for adsorption equilibrium assessment. The study showed that (Fe-Co)/BDC has a notable capacity towards of about 588 mg.g–1 for Cr-oxyanions contamination. Breathing effect is suggested to have a function to adsorption mechanism especially for the internal adsorption sites.***

Keywords: ***MOF, Breathing, ion exchange, wastewater treatment, Cr(VI) removal***

1 Introduction

Water pollution is a worldwide environmental worry and wide research attentions have been focused on the deletion of pollutants from wastewater [1]. Some pollutants are extremely dangerous and a type of these is the chromium oxyanions which are highly toxic contaminants with reasonable widespread due its use as for wood preservation, antifouling agent in cooling towers, pigments, metal plating, textiles, and leather tanning, etc. [2].

Accordingly, its concentration within several environment bodies, especially in water masses, has significantly increased during the last three decades [3]. Two abundant forms of chromium are known, Cr (III) and Cr (VI), where the later is toxic and carcinogenic [4]. It affects both human kidney and liver and origins dermatitis and diarrhea [5]. Referring to WHO, its permissible level in surface water is 0.05 ppm wherein in industrial wastewaters the concentration varies from 0.5 to 270 ppm [6]. Thus, it is essential to treat the chromium wastewaters. Various methodologies have been employed for the removal of inorganic metal ions contamination, including ion exchange [7], adsorption [8], or even photocatalytic degradation [9]. Ion-exchange is cost-effective and eco-friendly technique since it usually offers several advantages in terms of simplicity of operation, selectivity, and sensitivity [10]. In general, ion exchange can be classified as inorganic-based and organic-based. For inorganic type, the applied ion exchangers such as zeolites depend on their small pore size and thus exchange kinetics is not that fast to fulfill rate requirements, as well as limited adsorption capacity [11].

Although organic type, such as sol-gel materials and polymeric resins, are quick operating ion-exchangers, they are, unlike inorganic type, not of suitable thermal and chemical stabilities [12, 13].

Hence, the continue of developing a higher-performance ion exchangers for water treatment is a challenge however is a need. In this study, a metal organic framework (MOF) material is used as an adsorbent for chromium oxyanions to

remediate synthetic wastewater. Generally, a MOF material is a construct formed from metal ions as nodes which connected by organic linkers. The structures of most of these MOFs are characterized being porous which is a prime demand for effective adsorption process [14]. MOFs are known of their low densities, high surface areas, tunable pore size, and high porosities [15]. Hence, MOFs have been widely studied in various adsorption applications such as gas separation [16], gas adsorption and storage [17], catalysis [18] , adsorption of organic molecules [19], sensing [14, 20] and drug delivery [21].

Accordingly, adsorptive removal of organic and inorganic contaminants has become one of the most important research areas of MOFs where their adsorption capabilities are await to explore compared to the other adsorbents such as zeolites and activated carbon [22]. In addition, regeneration of MOFs, compared to activated carbon and zeolite which requires high temperatures and cost, could be of be simple processing [23]. All these advantages make it possible to candidate MOFs as potential efficient-adsorbents.

In this study, a MIL-53 from, the bimetallic (Fe-Co)/BDC, was selected as the MOF to apply for the removal of an inorganic contaminate, the chromium oxyanions. This MOF has shown a successful application for photocatalytic removal of organic contaminates [24]. However, unlike other MOFs, (Fe-Co)/BDC does not show considerable permanent high surface area. Because of its flexible structure, its pores opens only in the presence of incoming molecules, i.e. breathing feature [25]. The MOF structure consists of Fe(III)Co(II)(OH)(1,4-BDC) which is a distinctive class of MOFs produced by a combination between Fe(III)/Co(II) and 1,4-dicarboxylic acid [24]. The main advantages of using iron/cobalt as a bimetallic node system is to enhance the flexibility of the MOF to afford an ion exchange mechanism to remove dichromate ion from wastewater [24]. The aims of this work are: (1) to synthesize and characterize (Fe-Co)/BDC (2) to study the adsorption interaction and mechanism between (Fe-Co)/BDC and dichromate ion in aqueous solution.

2. Experimental

2.1. Materials and preparation of (Fe/Co)-BDC

Iron chloride ($FeCl_3.6H_2O$, 98%), cobalt chloride hexahydrate ($CoCl_2.6H_2O$, 99%), 1,4 benzene dicarboxylic acid (H_2BDC,98 %), and N,N-dimethylformamide (DMF, 98%) are all from sigma Aldrich and they were used for the synthesis of (Fe-Co)/BDC. Potassium dichromate ($K_2Cr_2O_7$, 99%, Alfa Aesar) was used to synthesize the synthetic chromium solutions by DI water. HCl and NaOH were used for pH adjustment and absolute ethanol was used for washing and regeneration purposes.

Samples of (Fe-Co)/BDC were synthesized through in-order addition of $FeCl_3.6H_2O$ (0.135 g, 0.5 mmol), $CoCl_2.6H_2O$ (0.115 g, 0.5 mmol) 1,4-benzendicarboxylic acid (H_2BDC) (0.166 g, 1 mmol), and acetic acid (1 mL) into a beaker. Then, N,N-dimethylformamide (DMF, 20 ml) was added and complete dissolving of content were recognized [24]. The produced solution was poured into a vial, and the vial was closed tightly and placed in conventional oven at 100^{o}C. The reaction was allowed to proceed at this temperature for about 6 hours where the resulting brown powder, (Fe-Co)/BDC, were collected by centrifugation at 6000 rpm for 30 minutes. The powder was then rinsed three times with DMF, acetone, and finally DI water. The washed powder were placed into an oven set at 140^{o}C overnight to dry.

2.2. Characterization of (Fe-Co)/BDC

The synthesized (Fe-Co)/BDC was characterized for chemical structure via: (i) FTIR (Jasco FT/IR 4100, KBr pellet method) and (ii) Raman (Model Sentera, Bruker, Germany). For crystalline nature, powder X-ray diffraction (PXRD, Shimadzu XD-l) was employed. For surface morphology and elemental composition, (i) SEM/EDX (Zeiss EVO-10 microscopy), and (ii) X-ray photoelectron spectrum ((XPS),

with a monochromatic Al-K_α 1486.7 eV (Thermo Fisher Scientific, USA)) were applied. For surface area determination, BET analysis (N_2 adsorption, NOVA Station A) was applied.

2.3. Adsorption experiments

Dichromate aqueous solutions of different initial concentrations were prepared (5, 10, 25 and 50 ppm) by dissolving required amounts in 50 ml DI water. All adsorption experiments were performed by batch method with some conditions were kept fixed: (i) temperature (ambient ~20ºC), (ii) sample shaking rate (100 rpm), and (iii) pH of dye solution (5.3 ± 0.02) to fulfil the isoelectric condition of (Fe-Co)/BDC surface to avoid probable buffering [26]. A specified amount of (Fe-Co)/BDC (0.05 g) was always used for each adsorption experiment. To observe adsorption propagation for each adsorption experiment, every 5 minutes (for an hour) a liquor sample of 3 ml was withdrawn from adsorption flask and the absorbance was recorded at λ= 375 nm using Agilent UV-Vis Cary 60) and then the liquor volume was returned back to the flask [27].

3. Results and discussion

3.1. Characterization

In addition to characterization of pristine (Fe-Co)/BDC, Cr-oxyanion treated (Fe-Co)/BDC samples were also characterized using PXRD, EDX, FTIR, Raman, XPS to collect some qualitative understanding of adsorption nature.

Fig. 1(A) shows the SEM image of (Fe-Co)/BDC which obviously elucidates the octahedron morphological shape of crystals where particle longitudinal-size is of about 3-5 µm. EDX spectrum of (Fe-Co)/BDC and elemental content comprises Fe, Co, C, and O are shown in Fig. 2(A). According to the elemental mapping shown in Fig. 2(B),(C),(D),(E), distributions of elements within the sample are uniform and homogenous and Co appears to distribute randomly within the frameworks [28].

XRD pattern of (Fe-Co)/BDC is shown in Fig. 1(B) and recorded 2θ values are consistent with the single crystal data simulation in reported literature which indicates sucseful synthesis process [24]. In addition, this indicates that both Fe and Co elements are allocated randomly and equivalently within (Fe-Co)/BDC matrix. In General, the phenomenon of breathing significantly affects the XRD patterns of the phases through modifcation in the cell volume and symmetry [29]. The diffraction peak at 8.9° should be indexed to (200) plane of the MIL-53 structure. The peak shoulder at 10.1° in fresh prepared (Fe-Co)/BDC has a shifte to 10.8° in after-adsorption sample which suggests the breathing effect for the duration of the adsorption process where MIL-53 converts from closed pores (CP) to open pores (LP). This behaviour has been identified before in flexible MIL-53 and was related to departure of water [30, 31]. It is of importance to mention that bimetallic MOFs offers recognized flexibility compared to the single metal MOFs. Hence, the presence Co in the MIL-53 (Fe) structure enhanced the breathing effect throughout adsorption process [32, 33].

The Raman spectrum of the (Fe-Co)/BDC is shown in Fig. 1(C) and where the peaks at 1605 and 1420 cm^{-1} are in accordance with the stretching modes of the carboxylate group. Furthermore, the three peaks at 1140, 860, and 629 cm^{-1} represent C–H bond produced from the benzene ring in the sample. The peak at 464 cm^{-1} should disclose the existence of M–O in the structure of (Fe-Co)/BDC. The same sample with some consecutive adsorption/regeneration cycles, shows as very similar spectrum to that of pristine one and this should point toward a physical adsorption process of dichromate onto (Fe-Co)/BDC.

FTIR spectrum of (Fe-Co)/BDC is shown in Fig. 1(D). The spectrum comprises two strong peaks at 1377 and1585 cm^{-1} which, respectively, are associated to the characteristic antisymmetric and symmetric O–C=O stretching frequency vibrations. The two peaks at 748 and 3422 cm^{-1} are also

recognized as for C–H bonding vibration and the O–H stretching mode of the benzene ring, respectively. Importantly, the peak at 543 cm^{-1} should be attributed to the metal–oxygen bond vibration (ν(M–O)) to represent the interactions between the carboxyl group of terephthalic acid and Fe/Co atoms [34].

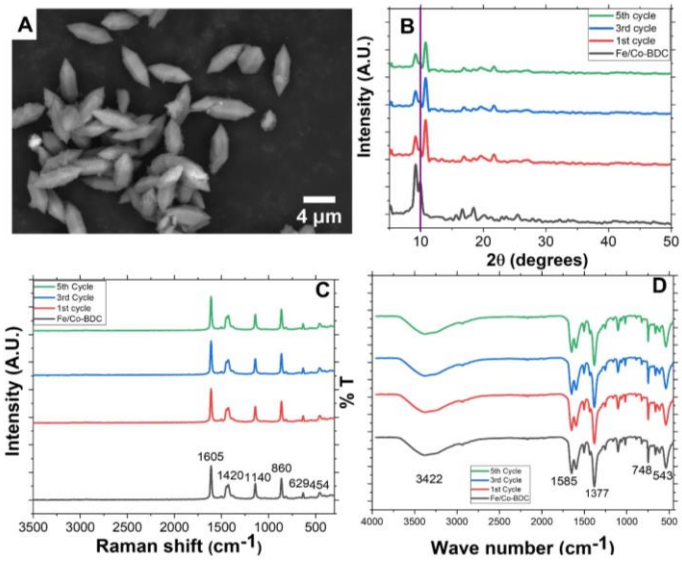

Fig. 1. (A) SEM image of (Fe-Co)/BDC, (B) XRD patterns, (C) Raman spectra, and (D) FTIR spectra of the pristine sample and after desorption/adsorption three selected cycles.

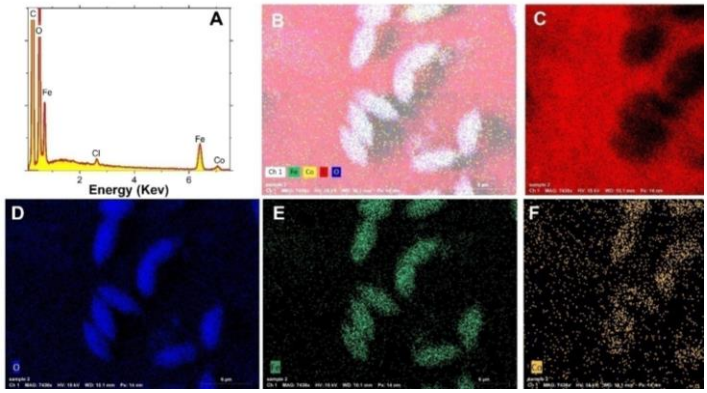

Fig. 2. (A) EDX spectrum, and (B), (C), (D), and (E) elemental mapping of (Fe-Co)/BDC.

3.2. Adsorption performance

The pristine (Fe-Co)/BDC is distinguished being comprising chloride, Fig. 3a, and this should be a substitution of hydroxyl groups [35]. The chloride, as substituent, is greatly dedicated to being exchangeable. To perform a verification of such anion exchange process, an extra EDX analyses have been conducted for (Fe-Co)/BDC after Cr-oxyanion adsorption and another more one after regeneration by NaCl solution, Fig. 3a and Fig. 3b. It is believed that chloride ion is responsible for Cr-oxyanions removal via an anion-exchange mechanism. Form Fig. 3b, after treating pristine (Fe-Co)/BDC with Cr-oxyanions solution, Cr appears at the complete expenditure of Cl. Then, after treating the sample with the regenerating solution for about 1 hour, NaCl (1M), Cl appears again at some expense of Cr (not shown). Obviously, this must be an anion exchange process. It is important to mention that upon regeneration, Cl^-/Cr-oxyanion exchange is not that complete and this could be due to the large size Cr-oxyanions which may requier more time for completeness. Also, the Lewis acid/base or coordination interaction between the oxygen of Cr-oxyanions with the unsaturated metal sites (open metal form) can explain the non-completeness of regeneration. To best of our knowledge, this should be the first anion exchange process presented by a MIL-35 material.

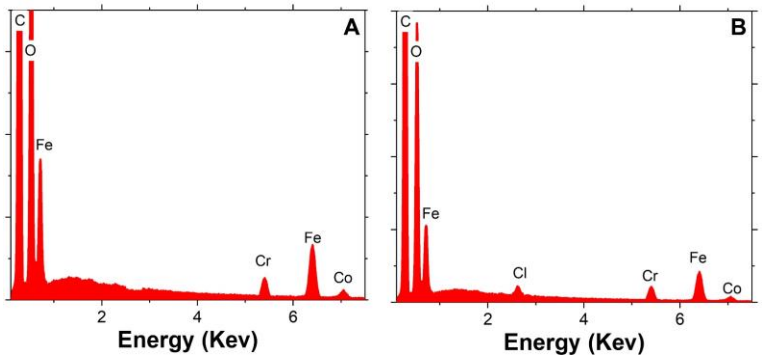

Fig. 3. EDX analysis results for (a) $Cr_2O_7^{2-}$loaded (Fe-Co)/BDC and (b) NaCl-treated (Fe-Co)/BDC.

Identification of a suitable pH value for an adsorption process is crucial for both the successful removal of the adsorbate and for more thoughtful of the process. Zeta-potential analysis was conducted for (Fe-Co)/BDC, via applying final pH vs. initial pH method, and pH_{PZC} was determined to be about 5.3 [36]. Adjusting adsorption Cr-oxyanions/(Fe-Co)/BDC system at

pH 5.3 provides the isoelectric surface of (Fe-Co)/BDC and denotes speciation of Cr-oxyanions as $Cr_2O_7^{2-}$, $HCrO_4^-$ and $CrO_4^{2-}$and most of which is $Cr_2O_7^{2-}$ [37].

The changes of the adsorbed amount of Cr-oxyanions, q, with time for the different initial concentrations are shown in Fig. 4. From the figure, for all C_i values it is obvious that a fast uptake occurred initially as the immediate steep increase of q occurs within the first period (PI stage) which expanded over only 3-5 minutes and then a period of a relaxed adsorption increase (PII stage) follows the first period which covers time-span that increases with C_i.

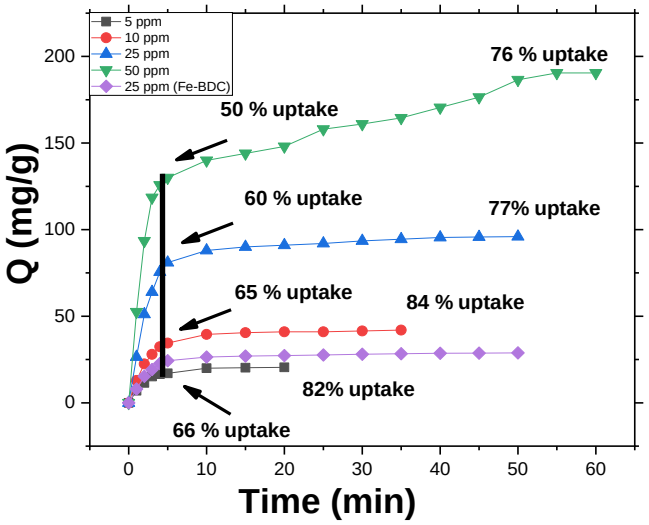

Fig. 4. change of $q_{exp.}$ with time for the different initial concentrations at room temperature 25 °C.

The immediate steep increase of q, as a phenomenon, indicates the strong affinity of (Fe-Co)/BDC towards Cr-oxyanions which should be contingent on some favouring strong physical/chemical interactions with the external surface of (Fe-Co)/BDC and abundance of its recipient sites. This phenomenon has an analogous in some preceding studies. As an example, 2,4-dichlorophenoxyacetic was exchanged with Cl^- using the MOF MIL-101(Cr)-Cl where the first fast adsorption stage of that study expanded over 100 minutes from a whole adsorption period of 1000 minutes and 82% of total uptake has been achieved for the highest applied initial concentration during this period [38].

Considering the PI stage, although q increases with C_i, the uptake percentage decreases, generally, returning the strong dynamic reversibility of the adsorption process. This reversibility is also manifested by the same performance of the PII stage where equilibration is preserved eventually. The strong dynamic reversibility definitely implies the readiness of (Fe-Co)/BDC structure for anionic exchange.

The endpoints of the PI stage (and the start of the PII stage) are evidently is the same for all C_i, from fig. 4., keeping in mind that the PII stage is accountable for adsorbing of 19, 18, 23, and 32% of total adsorbed amounts for C_i 5, 10, 25, and 50 ppm respectively. Certainly, the recipient sites on the outer surface of (Fe-Co)/BDC particles are partial compared to internal recipient sites and hence PII stage should start earlier for higher C_i. Even if, however, the outer surface of (Fe-Co)/BDC particles is not that limited, and the PII stage should be of delay-start for higher C_i. Hence, it is suggested that the reason for this resemblance of starting time of PII stage is that outer recipient sites are very plentiful considering the applied concentration range, 5-50 ppm. In addition, not only the initial concentration Cr-oxyanions is a driving force of adsorption but also the (Fe-Co)/BDC structure has a strong attractive environment for these anions with very appropriate pore size. Nevertheless, the abrupt transition from rapid adsorption, PI stage, to relatively relaxed one, PII stage, should originate from a significant diffusion action. As well, the general increase of q, during the PII stage, with C_i indicates the significant contribution of diffusion, especially for the higher C_i values.

Referring to (Fe-Co)/BDC structure, the readily Cr-oxyanions/Cl^- exchange can be suggested to have effect, during the PI stage, inside the very superficial layers. The outward migration of Cl^- ions should be immediate due to

proposed weak bonding within (Fe-Co)/BDC matrix and because of its small size compared to that of Cr-oxyanions. After interacting within the very superficial layers, Cr-oxyanions simply start to migrate inward during the PII stage through (Fe-Co)/BDC channels and steadily replacing Cl^- making use of breathing mode of flexible(Fe-Co)/BDC [39]. For effective Cr-oxyanion/Cl^-exchange, both the anions have to have the chance to migrate without considerable restraint within (Fe-Co)/BDC matrix which belongs to the MIL-53 MOF-type whose flexibility stems from the mutual effect of the metal node and the linker molecule [25]. It is worth to mention that Fe-BDC shows lower adsorption capacity compared to Fe-Co/BDC as stated in Fig. 4 for 25 ppm (70% less in adsorption capacity).

3.3. Adsorption kinetics and isotherms

For more understanding and proper assessment of the adsorption process, kinetic modelling and isotherm modelling were conducted. Both can shed light on the adsorption mechanism. Pseudo-first-order (PFO) and pseudo-second-order (PSO) kinetic models are frequently applied for studying the collective rate of adsorption. These models reflect the physical and/or chemical binding interaction(s) between solute and the active sites of the adsorbent. Both models present the dependency of adsorption rate on the availability of active sites on the surface of the adsorbent regarding solute concentration [40, 41]. It is not usual practice to apply PFO through stages; nevertheless, it could be advantageous to apply such a method for better understanding the adsorption process. Staged PFO modelling for the different initial concentrations, C_i is shown in Fig. 5. Brief inspection of PI stage points to the following: (i) fitting for the PI stage is accepted due to high values of R^2, (ii) $q_{PFO\text{-}PI}$ value strong-positively diverges from $q_{exp\text{-}PI}$ value, i.e. PFO modelling over-estimates $q_{PFO\text{-}PI}$ with respect to $q_{exp\text{-}PI}$, as C_i increases and this divergence indicates the conformity of PFO-adsorption process with low concentrations of Cr-oxyanions, and this means that external active sites are highly abundant for low concentrations, and (iii) the model-estimated rate constants are almost of the same value, around *ca*. 0.33, (which is not accostemed for adsorption processes) and this means that most of the adsorption events taking place during this period should be with the external sites. Hence rate constants are very similar which follows the basics of kinetic science. Considering the PII stage, fitting is generally less appropriate compared to that of the PI stage, regarding R^2 values, and hence adsorption process should not be controlled, solely, by Cr-oxyanions concentration. $\Delta q\%$ decreases obviously with C_i which contradicts the expectation of being increasing relation. Hence, PII stage does not follow PFO model and/or another adsorption mechanism other than exchange should has a contribution. The other mechanism, as a suggestion, could be the coordination of Cr-oxyanions via oxygen atom with some unsaturated nodes' metals of Fe-Co/BDC structure [37, 42]. In addition, the rate constants, $k_{PFO\text{-}PII}$, are neither similar to those of PI stage nor have a fashion with C_i. This also presents no suitability of the PFO model for PII stage. This is accepted as Cr-oxyanions concentration in this stage became low enough to affect the rate besides recipient sites. In general, though, it could be deduced that PFO-model is successful in representing the adsorption process for PI stage.

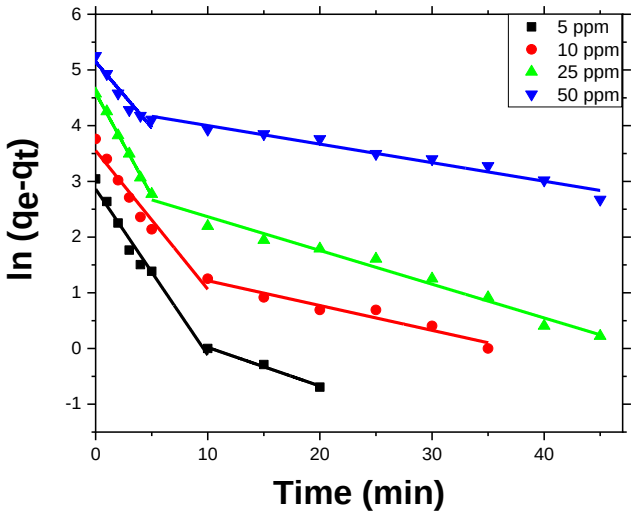

Fig. 5. PFO modelling of $Cr_2O_7^{2-}$ adsorption by (Fe-Co)/BDC.

PSO modelling for the different initial concentrations is shown in Fig. 6. As commonly observed for many adsorption

systems, this model has a remarkable good fitting for the different initial concentrations. This results from the ability of the PSO model to represent both physical and chemical adsorption processes [43]. values of q_{PSO} are in good agreement with values of q_{exp} as $\Delta q\%$ values conclude. values of k_{PSO} remarkably regularly decreases with C_i which points to the extended capacity of (Fe-Co)/BDC towards Cr-oxyanions over the applied concentration range. Also, this points to the reversibility nature of the adsorption process that is valid for both chemical and physical processes [43]. The change of k_{PSO} with C_i has also been presented in many other studies and it was a decrease relation in most cases and this relation has been verified experimentally and theoretically [40].

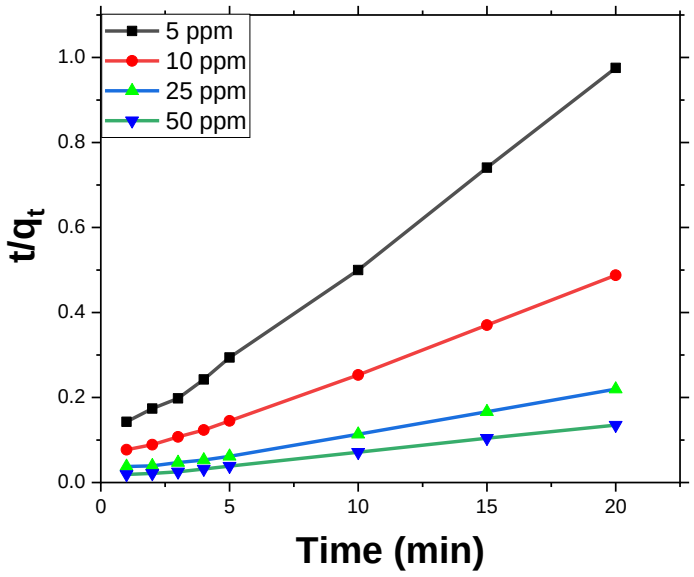

Fig. 6. PSO modelling of $Cr_2O_7^{2-}$ adsorption by (Fe-Co)/BDC.

Both of PFO and PSO models have no ability to illustrate the role of diffusion mechanisms in adsorption processes [40]. Therefore, there is all the time a need to apply models that consider the diffusion steps. Obviously, diffusions steps are necessarily attend any adsorption process when using porous materials. Here, DB-model was applied according to the staging approach as Fig. 7 shows. The DB-model depicts the experimental data for the different C_i, where the selected n=0.55 gave the best fitting [40, 41].

As for PFO modelling, the two periods, PI and PII, were considered. For the PI stage, the fittings according to R^2 values are accepted and suggest that a diffusion step engaged during this period even though the period is of very short time-period. As a result, the film diffusion can be suggested to contribute where adsorption occurs on the outer surface using the first layer of material. The channel opening event is not eagerly required, and anion exchange happens with external nodes and it can be suggested that (Fe-Co)/BDC surface is naturally polarized. Values of q_{DB-PI} agree sufficiently with the corresponding values of q_{exp-PI}, especially for low C_i, although with slight negative divergence as C_i increases and this is similar to PFO-modeling, yet with under-estimate. This divergence type should reflect the dependency of adsorption on Cr-oxyanions for low C_i values. These divergences indicate that both modelling types are required for the best representation of the adsorption process. Values of k_{DB-PI} increases regularly with C_i which is in agreement with PSO-modeling and suggests the increase of solute passage under the power of concentration difference as a driving force [40, 44].

For the PII stage, fitting is generally less proper contrast to that of the PI stage (may be except for the case 50 ppm) which is similar to PFO-modeling. Values of $\Delta q\%$ do not change regularly with C_i indicating different diffusion performances. As well, values of k_{DB-PII} do not properly change with C_i inferring also different diffusion performances. In general, it could be deduced that the DB model successfully represents the adsorption process for the PI stage.

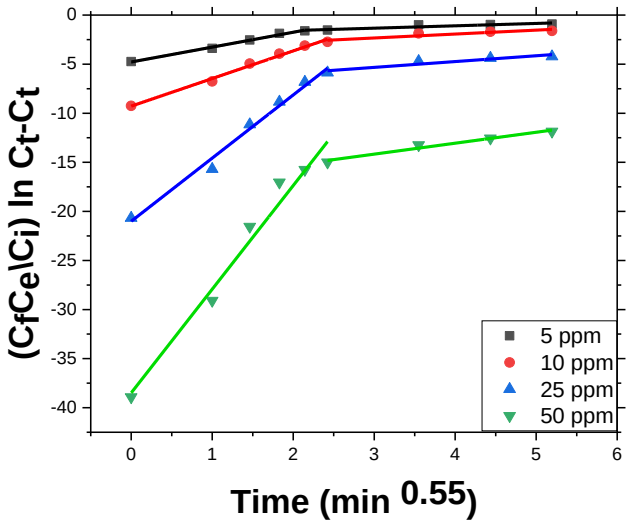

Fig. 7. DB-model modelling of $Cr_2O_7^{2-}$ adsorption by (Fe-Co)/BDC.

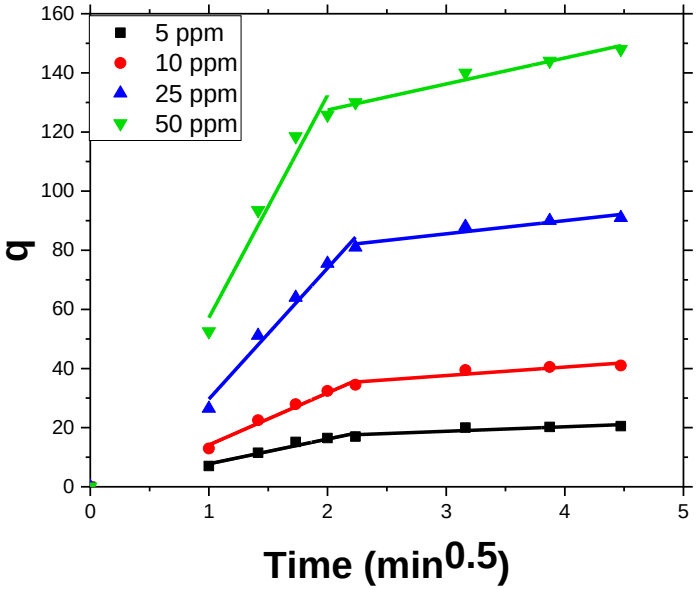

Fig. 8. WM-model modelling of $Cr_2O_7^{2-}$ adsorption by (Fe-Co)/BDC.

Considering the WM model, Fig. 8 shows its dipection of the experimental data for different C_i. As for DB-modelling, two stages were considered covering the same periods. For the PI stage, values of R^2 are very acceptable, however values of $q_{WM\text{-}PI}$ are that matching with $q_{exp\text{-}PI}$ compared to corresponding $q_{DB\text{-}PI}$, except for C_i= 50 ppm. Values of $k_{WM\text{-}PI}$ increase regularly with C_i same as $k_{DB\text{-}PI}$ which supports the proposal of the importance of film diffusion as DB-Model implies. For the PII stage, values of R^2 are generally acceptable for C_i= 25 and 50 ppm, however, the corresponding $q_{WM\text{-}PII}$ values are distant from $q_{exp\text{-}PII}$. Values of $k_{WM\text{-}PII}$ increase regularly with C_i same as $k_{DB\text{-}PI}$ support the proposal of the importance of pore diffusion.

Adsorbent capacity and interaction type towards certain adsorbate can be suggested by studying adsorption isotherm. Freundlich parameters, K_F and n, are related respectively to the adsorption capacity and intensity. Freundlich model considers multi-layer adsorption phenomenon and/or more than one binding mechanism, i.e. energy-heterogeneity of the adsorbent surface towards the targeted solute. Langmuir model assumes saturated mono-layer adsorption, homogeneous adsorbent surface and inhibition of migration of adsorbate over the adsorbent surface. Q_o (mg.g^{-1}) is the maximum adsorption capacity and b (l mg^{-1}) is related to adsorption-energy.

Fig. 9(a) and (b) elucidate respectively the Freundlich and the Langmuir modelling of experimental isotherm data. Referring to R^2 values, both models should satisfactorily represent the isotherm which is an indistinct case. Hence, engagement of more than one adsorption mechanism should be regrded and departure of water molecule could be considered as well. The obeying of data to Freundlich model presumes the participating binding mechanisms are anion exchange and coordination of Cr-oxyanions via oxygen atoms with positive

nodes [45]. with a contribution of diffusion steps. According to Langmuir modelling outputs, the maximum capacity of (Fe-Co)/BDC towards Cr-oxyanions is of a considerable amount, 588mg. g^{-1}, and this also indicates the enrolment of more than one mechanism. Compared to other some distinguished selected MOFs, (Fe-Co)-/BDC is extremely capacitive towards Cr-oxyanions.

4. Conclusions

Mechanism Cr-oxyanions/(Fe-Co)-/BDC adsorption system can be attributed to two steps. The first is anion exchange process through which the fast exchange of Cl^- ions with the hydrated $Cr_2O_7^{2-}$ ions takes place due to the abundancy of the well-distributed Cl^- on the upper surface of the (Fe-Co)/BDC. Second, after the fast complete coverage of the interactive surface layer, (Fe-Co)/BDC structure respond through breathing phenomenon to incubate adequately the adsorbed chromate ions and during this process (Fe-Co)/BDC rearrange inter-molecularly increasing the spacious molecular effect and modify the pores in (Fe-Co)/BDC this consequently creates a chance for further migration and physical adsorption for the rest of chromium anions in the contaminated solution as appeared in the second PII adsorption isotherm. It is suggested that breathing effect resulted in the Co-Fe positive nodes take effective positions after rearrangement of the orientation of the molecular lattice that functionally can attract more chromium anions.

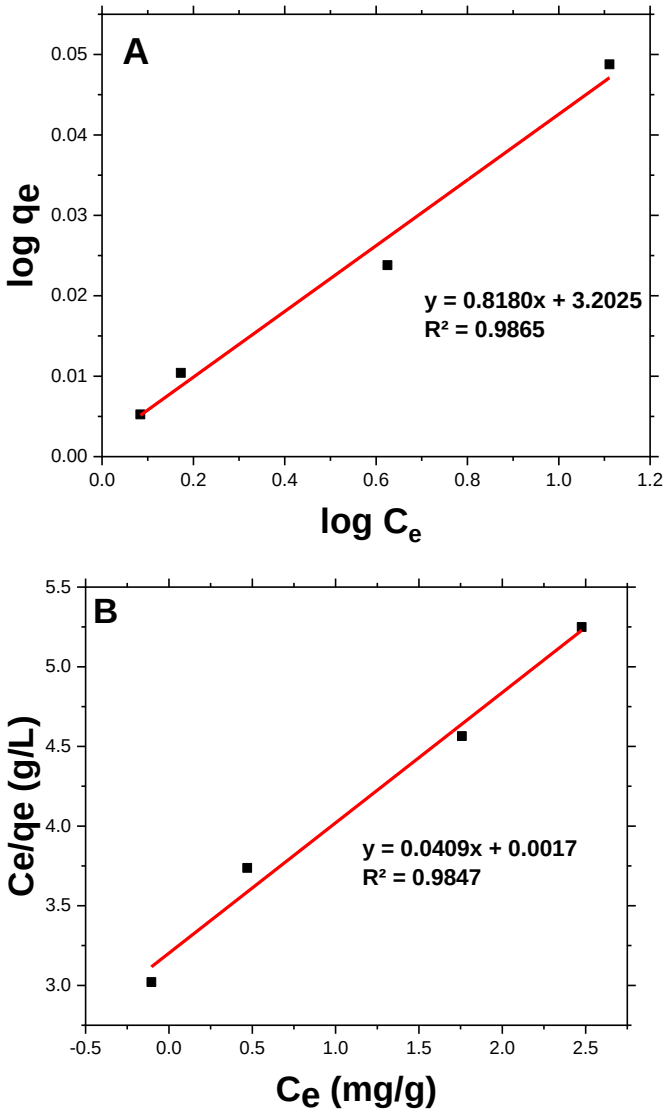

Fig. 9. Modeling of $Cr_2O_7^{2-}$ adsorption isotherm by (Fe-Co)/BDC, (a) Freundlich and (b) Langmuir

5 References

1. Rego, R.M., et al., *MOF based engineered materials in water remediation: Recent trends.* Journal of Hazardous Materials, 2020: p. 123605.
2. Singh, H.P., et al., *Chromium toxicity and tolerance in plants.* Environmental Chemistry Letters, 2013. **11**(3): p. 229-254.
3. Owlad, M., et al., *Removal of hexavalent chromium-contaminated water and wastewater: a review.* Water, Air, and Soil Pollution, 2009. **200**(1): p. 59-77.
4. Zhitkovich, A., *Chromium in drinking water: sources, metabolism, and cancer risks.* Chemical research in toxicology, 2011. **24**(10): p. 1617-1629.
5. Burrows, D., *Chromium: metabolism and toxicity*. 2019: CRC press.
6. Ghosh, P.K., *Hexavalent chromium [Cr(VI)] removal by acid modified waste activated carbons.* Journal of Hazardous Materials, 2009. **171**(1): p. 116-122.

7. Li, L.-L., et al., *Cr (VI) removal via anion exchange on a silver-triazolate MOF.* Journal of hazardous materials, 2017. **321**: p. 622-628.
8. Salgado-Gómez, N., M. Macedo-Miranda, and M. Olguín, *Chromium VI adsorption from sodium chromate and potassium dichromate aqueous systems by hexadecyltrimethylammonium-modified zeolite-rich tuff.* Applied clay science, 2014. **95**: p. 197-204.
9. Chen, S. and G. Cao, *Study on the photocatalytic reduction of dichromate and photocatalytic oxidation of dichlorvos.* Chemosphere, 2005. **60**(9): p. 1308-1315.
10. Luo, T., S. Abdu, and M. Wessling, *Selectivity of ion exchange membranes: A review.* Journal of membrane science, 2018. **555**: p. 429-454.
11. Schweich, D. and M. Sardin, *Adsorption, partition, ion exchange and chemical reaction in batch reactors or in columns—A review.* Journal of Hydrology, 1981. **50**: p. 1-33.
12. Luo, B., D. Yu, and J. Huo, *Polynuclear Cd (II) coordination polymer with unique configuration for chromium pollutants removal.* Journal of Solid State Chemistry, 2020. **283**: p. 121137.
13. Alexandratos, S.D., *Ion-exchange resins: a retrospective from industrial and engineering chemistry research.* Industrial & Engineering Chemistry Research, 2009. **48**(1): p. 388-398.
14. Abuzalat, O., *Synthesis and Characterization of Metal-Organic Frameworks Films and their Application as Chemical Sensors.* 2019.
15. Kitagawa, S., *Metal–organic frameworks (MOFs).* Chemical Society Reviews, 2014. **43**(16): p. 5415-5418.
16. Qiu, S., M. Xue, and G. Zhu, *Metal–organic framework membranes: from synthesis to separation application.* Chemical Society Reviews, 2014. **43**(16): p. 6116-6140.
17. Xu, J., et al., *Optimized synthesis of Zr (IV) metal organic frameworks (MOFs-808) for efficient hydrogen storage.* New Journal of Chemistry, 2019. **43**(10): p. 4092-4099.
18. Zhang, H., et al., *Engineering coordination polymers for photocatalysis.* Nano Energy, 2016. **22**: p. 149-168.
19. Liang, C., et al., *Aqueous Synthesis of a Mesoporous Zr-Based Coordination Polymer for Removal of Organic Dyes.* ACS Omega, 2019.
20. Abuzalat, O., et al., *Facile and rapid synthesis of functionalized Zr-BTC for optical detection of blistering agent simulant 2-chloroethyl ethyl sulfide (CEES).* Dalton Transactions, 2021.
21. Bera, S., et al., *Design and Synthesis of ZnII‐Coordination Polymers Anchored with NSAIDs: Metallovesicle Formation and Multi‐drug Delivery*. Chemistry‐An Asian Journal, 2020. **15**(4): p. 503-510.
22. Jiang, D., et al., *The application of different typological and structural MOFs-based materials for the dyes adsorption.* Coordination Chemistry Reviews, 2019. **380**: p. 471-483.
23. Kumar, P., et al., *Regeneration, degradation, and toxicity effect of MOFs: Opportunities and challenges.* Environmental research, 2019. **176**: p. 108488.
24. Li, H., et al., *Nanoporous bimetallic metal-organic framework (FeCo-BDC) as a novel catalyst for efficient removal of organic contaminants.* Environmental Pollution, 2019. **255**: p. 113337.
25. Schneemann, A., et al., *Flexible metal–organic frameworks.* Chemical Society Reviews, 2014. **43**(16): p. 6062-6096.
26. Mohsen, M., et al., *A cadmium-imidazole coordination polymer as solid state buffering material: Synthesis, characterization and its use for photocatalytic degradation of ionic dyes.* Journal of Solid State Chemistry, 2020. **289**: p. 121493.
27. Sanchez-Hachair, A. and A. Hofmann, *Hexavalent chromium quantification in solution: comparing direct UV–visible spectrometry with 1, 5-diphenylcarbazide colorimetry.* Comptes Rendus Chimie, 2018. **21**(9): p. 890-896.
28. Kim, D. and A. Coskun, *Template‐Directed Approach Towards the Realization of Ordered Heterogeneity in Bimetallic Metal‐Organic Frameworks.* Angewandte Chemie International Edition, 2017. **56**(18): p. 5071-5076.
29. Horcajada, P., et al., *Flexible porous metal-organic frameworks for a controlled drug delivery.* Journal of the American Chemical Society, 2008. **130**(21): p. 6774-6780.
30. Nouar, F., et al., *Tuning the breathing behaviour of MIL-53 by cation mixing.* Chemical Communications, 2012. **48**(82): p. 10237-10239.
31. Volkringer, C., et al., *XRD and IR structural investigations of a particular breathing effect in the MOF-type gallium terephthalate MIL-53 (Ga).* Dalton Transactions, 2009(12): p. 2241-2249.
32. Sapnik, A.F., et al., *Compositional inhomogeneity and tuneable thermal expansion in mixed-metal ZIF-8 analogues.* Chemical Communications, 2018. **54**(69): p. 9651-9654.
33. Chen, L., et al., *Bimetallic metal–organic frameworks and their derivatives.* Chemical Science, 2020. **11**(21): p. 5369-5403.
34. Gordon, J., H. Kazemian, and S. Rohani, *MIL-53 (Fe), MIL-101, and SBA-15 porous materials: potential platforms for drug delivery.* Materials Science and Engineering: C, 2015. **47**: p. 172-179.
35. Breeze, M.I., et al., *Isomorphous Substitution in a Flexible Metal–Organic Framework: Mixed-Metal, Mixed-Valent MIL-53 Type Materials.* Inorganic chemistry, 2013. **52**(14): p. 8171-8182.
36. Jung, B.K., Z. Hasan, and S.H. Jhung, *Adsorptive removal of 2, 4-dichlorophenoxyacetic acid (2, 4-D) from water with a metal–organic framework.* Chemical engineering journal, 2013. **234**: p. 99-105.
37. Hatem, H., et al., *Buffering-like cationic coordination polymer AgM-CP for adsorptive removal of chromate anions from aqueous solution: Isotherm and thermodynamics.* Journal of Solid State Chemistry, 2020. **286**: p. 121271.
38. Chen, T., et al., *Preparation of cationic MOFs with mobile anions by anion stripping to remove 2, 4-D from water.* Materials, 2017. **10**(8): p. 879.
39. Yılmaz, E., E. Sert, and F.S. Atalay, *Synthesis, characterization of a metal organic framework: MIL-53 (Fe) and adsorption mechanisms of methyl red onto MIL-53 (Fe).* Journal of the Taiwan Institute of Chemical Engineers, 2016. **65**: p. 323-330.
40. Baraka, A., *A novel kinetic model for batch aqueous-solution/porous-solid adsorption systems.* Desalination and Water Treatment, 2014. **52**(28-30): p. 5343-5356.
41. Baraka, A., *Investigation of temperature effect on surface-interaction and diffusion of aqueous-solution/porous-solid adsorption systems using diffusion–binding model.* Journal of Environmental Chemical Engineering, 2015. **3**(1): p. 129-139.
42. Kökçam-Demir, Ü., et al., *Coordinatively unsaturated metal sites (open metal sites) in metal–organic frameworks: design and applications.* Chemical Society Reviews, 2020. **49**(9): p. 2751-2798.
43. Baraka, A., *Adsorptive removal of tartrazine and methylene blue from wastewater using melamine-formaldehyde-tartaric acid resin (and a discussion about pseudo second order model).* Desalination and Water Treatment, 2012. **44**(1-3): p. 128-141.
44. Nouri, L., et al., *Batch sorption dynamics and equilibrium for the removal of cadmium ions from aqueous phase using wheat bran.* Journal of hazardous materials, 2007. **149**(1): p. 115-125.
45. Zhang, L., et al., *Synthesis of titanium cross-linked chitosan composite for efficient adsorption and detoxification of hexavalent chromium from water.* Journal of Materials Chemistry A, 2015. **3**(1): p. 331-340.